Journal of Applied Polymer Science

Preparation, Properties, and Applications of Acrylic–Polyurethane Hybrid Emulsions in Extinction Electrophoresis

Juhua Ou,[1,2] Yong Yang,[1,2] Jianqun Gan,[1] Chengyong Ha,[1,3] Min Zhang[1,3]

[1]Guangzhou Institute of Chemistry, Chinese Academy of Sciences, Guangzhou 510650, China

[2]University of Chinese Academy of Sciences, Beijing 100049, China

[3]Laboratory of Cellulose and Lignocellulosics Chemistry, Chinese Academy of Sciences, Guangzhou 510650, China

Correspondence to: M. Zhang (E-mail: zhangmin@gic.ac.cn)

ABSTRACT: Aqueous acrylic–polyurethane hybrid emulsions (PUA) were fabricated by semibatch emulsion copolymerization using a mixture of acrylic (AC) monomers in the presence of an isocyanate terminated polyurethane (PU). The effects of PU content on the morphology of the hybrid emulsions and film properties were here investigated in detail using FT-IR, UV, TEM, and SEM. TEM images clearly showed that hybrid emulsions exhibited a core-shell structure before neutralization. However, after neutralization with *N*,*N*-dimethylethanolamine, the typical particles exhibited phase inversion, producing particles with irregular hemispheres shapes and diameters about 0.5 μm. SEM images showed that the film surface became rougher as PU content increased, peaking at 10 wt %, the gloss of this film was 23.1 (60°). The UV transmittance spectra of the PUA hybrid emulsion within a wavelength range 700–200 nm decreased as PU content increased. This was consistent with the changes in the surface roughness of the film. Electrophoresis took place on an aluminum alloy surface and the product was dried at 120°C. The film exhibited excellent mechanical performance due to curing reaction between the N═C═O group on PU and hydroxyl group on the AC copolymer. The gloss of the film was found to be as low as 4.0 after electrophoresis testing. These films may be useful in practical extinction electrophoresis. © 2013 Wiley Periodicals, Inc. J. Appl. Polym. Sci. **2014**, *131*, 40078.

KEYWORDS: applications; emulsion polymerization; electrochemistry; films; morphology

Received 29 May 2013; accepted 20 October 2013

DOI: 10.1002/app.40078

INTRODUCTION

Recently, for safety reasons and associated with health and environmental requirements, the coating industry has gradually transitioned its focus from solvents to water-dispersible materials. The use of waterborne polyurethane modified acrylic resin has drawn considerable attention from a wide range of scientific and practical viewpoints because these resins usually exhibit excellent performance and specific environmental advantages. In general, acrylic resins show excellent hardness and weather resistance, remarkable water and alkali resistance, and affinity to pigments, they can also be produced at little cost. However, they suffer from poor toughness, mar-resistance, elasticity, adhesion properties and softness, which are characteristic of polyurethane resins. So far, the incorporation of an acrylic component into PU dispersions has been widely studied by many research teams.[1–5] The combination of these two polymers gives the product novel properties.[6,7]

The usual methods of preparing polyurethane–acrylic hybrid emulsions (PUA) are direct blending of PU and AC dispersions (common physical mixing) and hybrid emulsion polymerization. PUA blends would exhibit low-quality performance unless the problem of compatibility between PU and AC was improved. An alternative approach to physically mixing acrylic and polyurethane dispersions is to form a dispersion of particles using *in situ* polymerization of the respective premixed monomers and prepolymers to form hybrid particles. The key to this process is that the polymerization mechanisms of these polymers are different, PU is formed through step-growth polymerization and AC is formed through free radical chain growth polymerization. For this reason, the AC and PU segments are not directly attached to each other by primary bonds.[8,9] The hybrid particles were held together with numerous entanglements and secondary intermolecular bonding forces to produce an interpenetrating network (IPNs) and the AC and PU components in the hybrids were mixed at the molecular level. Another method to produce PUA hybrids is miniemulsion process,[10] where the simultaneous addition polymerization of an isocyanate terminated PU and free-radical polymerization of a mixture of AC monomers can be carried out in this process. This

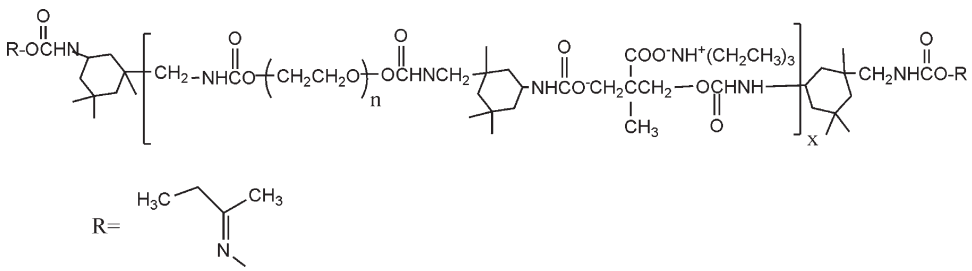

Figure 1. The structure of polyurethane.

method offers the possibility of compatibility between both polymers, resulting in a synergy of properties in the final product.

So far, most studies have focused on latex particles and morphology of the PUA hybrids and their applications in binders for paints, pressure-sensitive adhesives and special coating materials.[11–18] However, there are few reports concerning the surface gloss of the PUA films. Amalvy et al. described the production of glossy topcoat one-pot exterior paint formulations using water-based PU/AC hybrid binders.[19] They investigated the effects of the pigment to volume ratio and the amount of acrylic on the properties of the film, and found that the air-dried formulations based on hybrid PU/AC with up to 50 wt % acrylic component showed a level of gloss as high as 70. The relative gloss changed after accelerated weathering testing. It became lower than that of pure solvent-based AC and PU paints. Tu et al. investigated a two-component waterborne polyurethane comprised of water-soluble AC resin and HDI biuret.[20] They found the miscibility of water-soluble AC resin and HDI biuret is the key to prepare transparent, high-gloss films. More recently, the works of Gite et al. discussed the effects of NCO/OH ratio and an increase in hydroxyl content of acrylic polyols on the properties of polyurethane (PU) coatings.[21] Their experimental results revealed that all polyurethane coatings based on acrylic polyols and IPDI trimers showed good gloss, good scratch resistance, and excellent adhesion. Recently, Huang et al. discussed the preparation of hybrid systems using polyurethane/poly (*n*-butyl acrylate-styrene) emulsions with dimethylol propionic acid as a chain extender.[22] They investigated the influence of acrylic monomers and dimethylol propionic acid content on the physical properties of films intended for paper sizing applications. The gloss of the treated paper was considerably improved.

However, until now, no detailed studies on extinction performance during electrophoresis have been reported using PUA hybrid emulsions.

In this article, PUA hybrid emulsions were formulated using the semibatch emulsion polymerization method[23–25] with different concentrations of PU. In this emulsion, the isocyanate terminated PU polymers contained pendant carboxylic groups and methyl ethyl ketoxime end groups and the acrylic copolymers provide hydroxyl functionality. This facilitated compatibility between AC and PU polymers. These functional groups react with each other during the film formation process, which affects the level of gloss of the coating. Relative structure–property relationships, the surface properties of the dried films, and the electrophoresis behavior of these hybrid emulsions have been studied.

EXPERIMENTAL

Materials

Methyl methacrylate (MMA, 98%), methacrylic acid (MAA, 99%), butyl acrylate (BA, 99%), styrene (ST, 99%), triethylamine (TEA, 99%), and curing agent w-7130 (Enclosed water-based isocyanate crosslinking agent) were purchased from Jiangsu Yonghua Fine Chemicals, China. The 2-hydroxyethyl methacrylate (HEMA, 98%), potassium persulfate (KPS, 99.99%), sodium dodecyl sulfate (SDS, 99%) *N*,*N*-dimethylethanolamine (DMAE, 99%), isophorone diisocyanate (IPDI, 99%), dimethylolpropionic acid (DMPA, 98%), methyl ethyl ketoxime (MEKO, 99%), dibutyltin dilaurate (DBTDL), and polyethylene glycol (PEG, $M_n = 400$ g mol^{-1}) were purchased from Aladdin Reagent (Shanghai). Acetone was obtained from the Guangzhou Chemical Reagent Factory of China. All these materials were used without further purification. Deionized water was used for all polymerization and treatment processes.

Preparation of Aqueous Polyurethane Dispersion

The aqueous polyurethane dispersion was synthesized according to the literature[26] with slight modifications. In a four-necked round-bottom flask equipped with a mechanical stirrer and a reflux condenser, under nitrogen atmosphere, 31.75 mmol of PEG, 63.28 mmol of DMPA and 100.36 mmol of IPDI in the presence of catalyst DBTDL (0.1 wt % based on total solids) were added to the reactor. The temperature was raised to 80°C and stoichiometric amount of acetone was poured into the reactor. The reaction proceeded until the prepolymer had reached the expected amount of residual isocyanate groups, then 14.94 mmol of MEKO was added to it and stirred for 2 h to ensure complete reaction of isocyanate groups. After cooling the system below 60°C, 100.36 mmol of TEA was added and stirred for 1 h. The resultant polyurethane ionomer was then dispersed in water under vigorous stirring rate for 30 min and an anionic PU dispersion with a particle size of about 100 nm and 20% solid content was achieved. The structure of polyurethane is illustrated in Figure 1.

Synthesis of PUA Emulsion

Synthesis of PUA emulsion was carried out in a 500-mL round-bottom flask equipped with a mechanical stirrer, thermometer with a temperature controller, and additional funnels. Different amounts of PU (based on the total amount of solid AC) were

Table I. Typical Recipes for the Synthesis of PUA Emulsions

Materials	Part A (g)	Part B (g)
HEMA	1.67	3.34
MMA	2.14	4.28
MAA	1.06	2.12
St	1.40	2.80
BA	3.78	7.56
PU	4.52-22.61	0
Initiator (KPS)	0.0603	0.1206
Deionized water	202	0

dispersed in distilled water and charged to the reactor at 70°C. The monomers, initiator and deionized water, as indicated in Part A in Table I were charged into the flask and heated to 80°C within 30 min under constant stirring to obtain seed latex. Then the remaining AC monomers mixture and initiator solution as Part B showed in Table I were fed through an addition funnel over the course of 3 h. After the addition of all ingredients, the reaction mixture was maintained at that temperature for an additional 1 h to complete the reaction. Then the reaction mixture was cooled to 45°C and stoichiometric amount of *N*,*N*-dimethylethanolamine was added to neutralize the free carboxylic groups. A waterborne PUA hybrid emulsion with about 15% solid content by mass was produced.

Electrophoresis

To evaluate the electrophoresis of the PUA composite latex, W-7130 closing waterborne curing agent was added into the latex with 10 wt % PU content at 80°C in an apparatus equipped with reflux condensing for 1 h. The mixture was then cooled to 45°C. Then *N*,*N*-dimethylethanolamine was added to adjust the pH to 7.5–8.5. The reaction was allowed to continue for 30 min. The electrophoresis experiment proceeded on aluminum samples with an anode with 100–120 V for 120 s to obtain the insoluble film, the aluminum samples were cured at 120°C for 0.5 h. Figure 2 shows the curing reaction between PU and AC.

Preparation of Films

The polymer films were prepared by casting PUA emulsion into glass molds. They were dried at room temperature for 7 days and then at 50°C for 1 day. This trend of drying is just for slow drying to evaporate the water. After demolding, the films were stored in desiccators at room temperature for further study.

Characterization

Fourier Transform Infrared Spectroscopy (FTIR). The infrared spectra of PU and PUA were obtained on a RFX-65 A FTIR spectrophotometer in KBr. The spectra of dried PU and PUA films were collected within the range of 4000–400 cm^{-1}.

Particle Size Analysis. The particle size of PUA hybrid emulsion was measured using a laser light scattering method with a JL-1177 instrument. The measuring range of the instrument was 3–3000 nm. The samples had been diluted before the study began and were kept at 25°C during the measurement.

UV–Vis Spectra. A UV–vis spectrophotometer (UV-2550) was used to measure the transmittance spectra of the PUA emulsion latex within a wavelength range of 700–200 nm wavelength light.

Morphological Properties. The morphology of the PUA latex was obtained by transmission electron microscopy (TEM, JEM-100CX II). The samples were dried on carbon-coated copper grids, and phosphotungstic acid was used to stain the sample. The morphology of the PUA films was observed using scanning electron microscopy (SEM, JSM-6360LV), the dried films were stained on copper grids and gold was sprayed over the samples. Both sets of images were used to study the compatibility between PU and AC phases.

Thermal Analysis. The thermal curves of thermogravimetric analysis (TGA) were recorded using a PerkinElmer analyzer. The temperature ranged from room temperature to 700°C at a heating rate of 10°C min^{-1}, in a nitrogen atmosphere. Differential

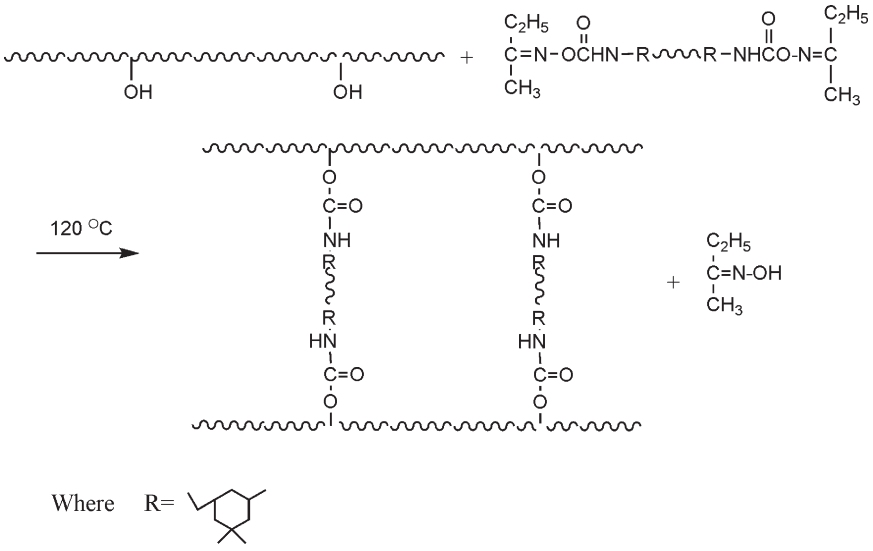

Figure 2. The curing reaction between PU and AC.

scanning calorimetry (DSC) was performed to characterize the thermal response properties of the PUA films. DSC was performed using a Mettler Toledo DSC821 instrument with nitrogen cell purification and heating rates of 20°C min^{-1} from −70 to 120°C.

Contact Angle. A DSA 10 video contact angle measuring device was used to measure the contact angle of the PUA films. Distilled deionized water was used as the reference liquid. About three independent measurements were made on different parts of the film, which had been dried at room temperature for 7 days by casting PUA onto glass slide. The average contact angle was reported.

Gloss. The gloss of dried PUA films was determined at 60° using a KGZ-60 gloss meter according to ASTM E 284. About three independent measurements were made on different parts of the film.

Mechanical Properties. Pencil hardness was determined using ASTM 3363. A crosscut adhesion was used as per ASTM D 3359-87 to study the adhesion.

Electrophoresis Properties. All the electrophoresis properties were checked on aluminum plate samples (60 × 100 × 2 mm^3). Film thickness was determined by SSPC PA2. Impact resistance was measured using ASTM D5420-10. Salt spray resistance (5% NaCl, 24 h) was evaluated by ASTM B117. Acid resistance was checked according to the ASTM D 1674-89, the aluminum samples were dipped into 3% (w/w) NaOH solution or 5% (w/w) sulfuric acid solution for 72 h and the corrosion rate of the samples are <0.05% of the area.

RESULTS AND DISCUSSION

Fourier Transform IR Spectra

By comparing the IR spectra with PU and PUA, pure AC was prepared according to the procedure PUA hybrid emulsion except using 3 wt % SDS as surfactant. Figure 3 shows the FTIR spectra of the dried films of PU dispersion, AC and the PUA hybrid emulsions. The FITR spectra of PU film shows that the absorption peak of NCO band at 2265 cm^{-1} disappeared, demonstrating that the polymerization reaction in PU dispersion was completed.

The PU and PUA spectra exhibit strong absorption bonds at 3338 and 3442 cm^{-1} (peaks a and a' in Figure 3), respectively, due to the N—H stretching vibration. The N—H stretching vibration of PUA shifted to the higher frequency, which may be ascribed to the formation of hydrogen bonds between PU and AC. The obvious shift of the C=O stretch in PUA spectrum

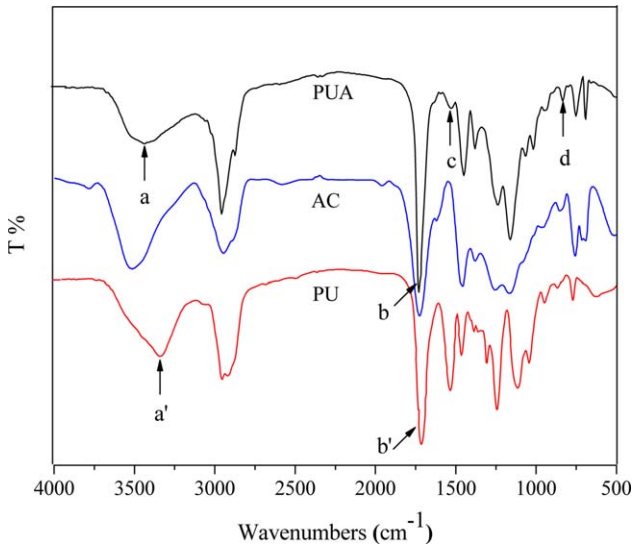

Figure 3. FTIR spectra of PU, AC and PUA with 10 wt % PU. [Color figure can be viewed in the online issue, which is available at wileyonlinelibrary.com.]

from 1716 to 1731 cm^{-1} (peaks b and b′ in Figure 3) can be attributed to the concentration of hydrogen bonds[27] which was ascribed to the presence of AC component. The spectrum of PUA presents a weak peak at 1540 cm^{-1} related to the stretching of C—N (peak c in Figure 3) can be attributed to the PU composite. The disappearance of the band at 1680–1620 cm^{-1} is attributable to the double bond and the emergence of sharp absorption at 844 cm^{-1} (peak d in Figure 3) can be assigned to the completion of reaction of polyacrylate. All these evidences confirmed that PU has been connected to the AC composite during the polymerization process.

Physical Properties

The physical properties of the PUA films are shown in Table II. As the PU content in the resin increased, the transparent PUA films became opaque. Gloss decreased from 84.0 to 22.2. When PU content increased up to 10 wt %, the matting film was formed.

Hybrid membranes with only a single T_g are described in Table II. For comparison, the pure PU and pure AC were detected to be about 16.91 and 19.50°C, respectively. The PUA hybrid emulsions exhibit only one T_g, which was higher than both PU and AC. The T_g values first increased slightly and then decreased as the PU content up to 10 wt %. The higher T_g of PUA hybrids was attributed to partial compatibility and

Table II. Physical Properties of PUA

No.	PU content (wt %)	Appearance	Gloss	T_g (°C)	Pencil hardness	Adhesion
1	3	Transparent	84.0	35.82	3 H	1
2	5	Transparent	74.3	37.68	4 H	1
3	7	Translucent	70.5	40.14	6 H	1
4	10	Opaque	23.1	39.51	4 H	2
5	15	Opaque	22.2	26.85	3 H	3

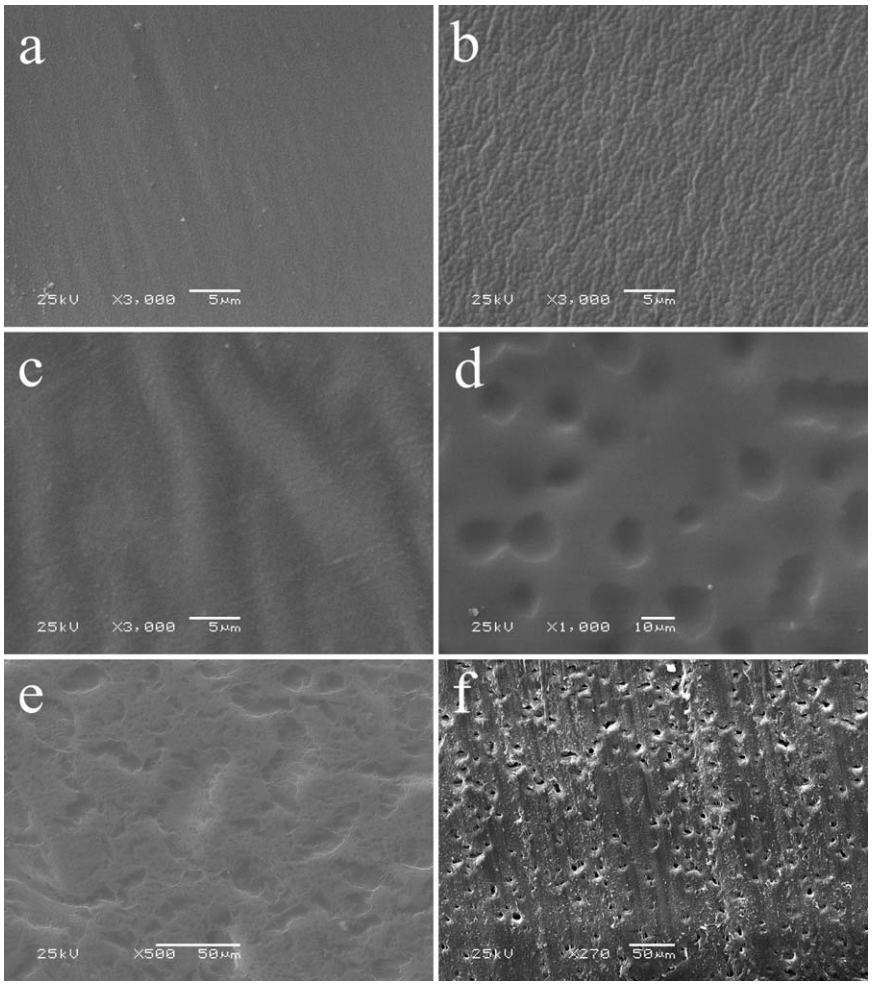

Figure 4. SEM of PUA hybrid membrane: (a) 3 wt % PU, (b) 5 wt % PU, (c) 7 wt % PU, (d) 10 wt % PU, (e) 15 wt % PU, (f) cross section of 10 wt % PU.

formation of network of intermolecular hydrogen bonds, achieving some degree of miscibility or grafting. Moreover, the methyl ethyl ketoxime groups can be released from the isocyanate terminated PU during the drying process and generates isocyanate groups, which is reactive toward the functional groups of AC, the crosslinking reaction occurred between the two components and a higher T_g values than the pure PU or AC is expected. On the other hand, as compared hybrids with 3–7 wt % of PU, levels of PU over 10 wt % showed lower T_g, it may be assumed that higher amount of the PU in the hybrids cause slight phase separation. The results of T_g measurements indicated some degree of miscibility between AC and PU, but it is difficult to conclude that the AC and PU have combined chemically at the molecular level because some portion of the PU component was grafted with AC and relatively very small amount of PU left in the PUA hybrid films and the AC component is dominate.[28] The further discussion on the morphology of the particles will clarify the interactions between the AC and PU phase.

The hardness and adhesion of PUA increased as PU content increased from 3 to 7 wt % owing to the good compatibility of the two systems that they bring to combine the positive properties of PU and AC in a synergistic way. However, PU is not very rigidity or thermally stable and has low thermal expansion coefficients.[29] Furthermore, because of the limited compatibility of the two systems, the incorporation of excess PU into the AC matrix leads to the production of polymer composites with lower glass transition temperatures and poor mechanical properties, such as pencil hardness and adhesion. Table II presents results showed that the best compromise in properties appears to be the sample with 10 wt % PU which combines an improvement in physical properties and gloss decrease in forming matting film.

Morphological Properties

The surface of PUA films made with different amounts of PU was investigated using SEM to evaluate the surface morphology. Results are summarized in Figure 4. They clearly show that surface roughness increases with elevated PU content, peaking at 10 wt %. In the case of 3 wt % PU [Figure 4(a)], the surface was homogeneous and smooth. When PU content increased, film surface roughness also increased [Figure 4(b,c)] and small concave structures formed [Figure 4(d,e)]. When a beam of light was cast on the uneven film, scattering phenomena occurs leading to a matting film.

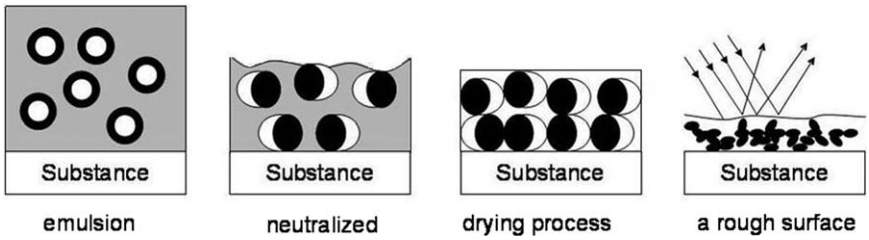

Figure 5. Film formation process of PUA composite latex with 10 wt % content PU.

Morphology is closely related to the interactions between AC and PU. Because of the compatibility of PU and AC, the crosslinking kinetics and phase separation kinetics are heavily competitive. When PU content is low, as shown in Figure 4(a–c), AC and PU form a homogeneous system through the formation of strong H-bonds between their polar groups, which can improve the comprehensive performance of the coatings. When PU content is high, as shown in Figure 4(d,e), the excess PU was not integrated into the crosslinked matrix. Instead, its chains acted like condensing agents which caused a less irregular surface. These irregular concave structures are due to the heterogeneities in the particle surface energy. During the polymerization process, the addition of MMA affects the particle morphology because MMA can promote homogeneous nucleation. In this case, homogeneous nucleation mechanisms and droplet nucleation could carried out simultaneously, resulting of heterogeneous distribution of PU in the particles, which leads to some degree of phase separation between AC and PU components.[10] The growth of the PUA network became entropically unfavorable and uneven volume shrinkage took place during the dry process in the film, which in turn increased the roughness of the film surface. Moreover, the PU containing anion leads to forming polymer electrolytes and created a porous structure.[30] Similar results regarding the gloss of the dried films are shown in Table II.

Following one proposed mechanism of 10 wt % PUA composite latex film formation explains this deformation which is illustrated in Figure 5. During the film formation process, particles interact with other particles and with the interface. Molecular interdiffusion of polymer chains takes place. The hydrophilic polyurethane phases tend to gather together and some of the acrylic phase orients near the substrate. Finally, a small amount of volume shrinkage and a rough surface film are achieved.

To explain these phenomena reasonably, the morphologies of PUA emulsion latex made with 10 wt % PU before and after neutralization with DMAE were observed using a transmission electron microscope. A typical unneutralized PUA emulsion latex is shown in Figure 6(a). The particles are approximately uniform spheres with an average size of 260 nm. Here, the lighter AC regions are the core and the darker PU domains are the shell. The PU domains became darker because of the dense electron clouds, which have more pronounced polarity than the AC chains. A typical neutralized emulsion latex is shown in Figure 6(b), the image shows that the neutralized emulsion particles (the average size is about 0.5 μm) tend to become much larger than the unneutralized ones. Furthermore, the particles were found to have irregular boundaries rather than regular, spherical shapes. The same irregular structure change was observed in past works.[31] It was demonstrated that the hybrid emulsions containing a hydrophilic core with carboxyl groups in alkalization treatment brings a great effect on the morphology of the particles. The DMAE could diffuse into the core particles and react with the carboxylated group in the AC composite, and the strong electronic cloud density of the AC chains appears to significantly increase, in this case it decreases the polarity gap between AC and PU and causes the carboxylated groups of AC to diffuse from the core side to the out side of the particles. After alkalization, the viscosity of the PUA latex system and interfacial tension of the particles were changed. Consequently systems like irregular hemisphere are often the most stable structure with respect to thermodynamic equilibrium. The results from the hybrid systems with 10 wt % PU

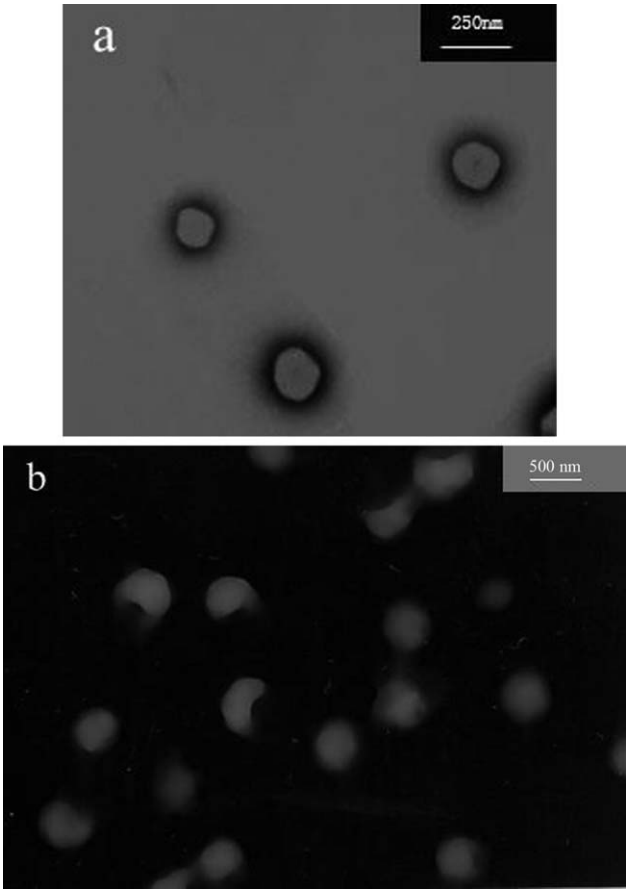

Figure 6. TEM images of PUA emulsion latex with 10 wt % PU (a) before and (b) after neutralization.

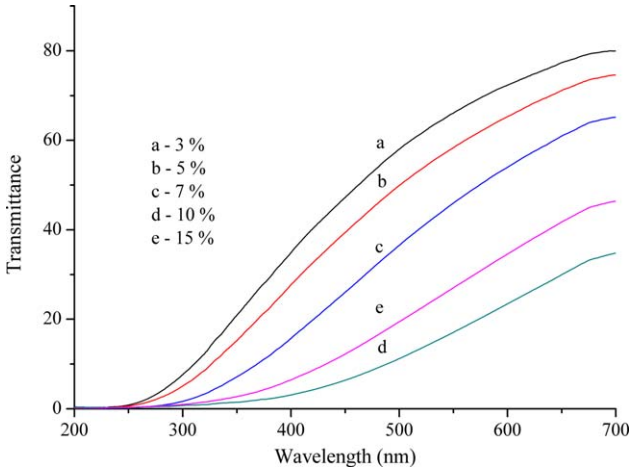

Figure 7. Transmittance spectra of PUA hybrid emulsions. [Color figure can be viewed in the online issue, which is available at wileyonlinelibrary.com.]

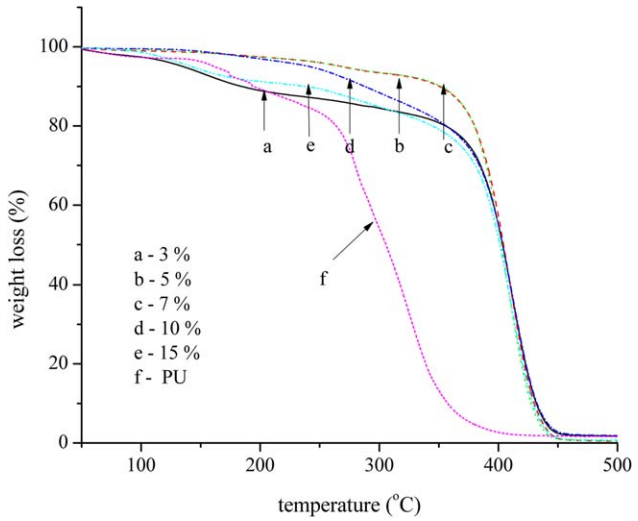

Figure 8. TGA curves of PUA and PU films. [Color figure can be viewed in the online issue, which is available at wileyonlinelibrary.com.]

identified the phase separation occurs leading to porous polymer film. On the other hand, phase separation of the hybrids is related to the polymer–polymer interfacial tensions. It is clear that PU acts as a surfactant in this hybrids and an increase in the fraction of the PU causes slight phase separation. It is in good agreement with the results of Sundberg.[32] They reported that the surfactant concentration could affect the interfacial tensions. In the case of low surfactant concentration, the interfacial tensions between the two polymers and the aqueous phase are high enough to form a core shell structure, but at higher concentrations, the polymer/water interfacial tensions appears to reduce and the polymer/polymer interfacial tension is highly influential in determining the morphology of the hybrid latex, resulting in lower free energy levels of the system. As compared with AC, PU has a lower molecular weight, it is also the more mobile phase, which provides a stronger driving force for the phase migration.[33] In this situation, systems like irregular hemispheres can be achieved.

The presence of MAA also affects the morphology of the structured of the latex particles. MAA contains a hydrophilic carboxylic group, which can affect the polarity of the polymer and change the polarity contrast between the two phases. For the PUA hybrids, the incorporation of MAA in the hybrids can increase the polarity of AC component and decreases the polarity contrast, suggesting some degree of miscibility. When the DMAE was added into the hybrid latex, the pH of the system raised and it offers possibility to let the water swell into the particles, it promotes the AC components to move to the outside of the particle, forming a hydrated polymer shell surrounding with a upswollen core,[32] indicating a higher interfacial area and higher free energy of the system, which may provide driving force for phase separation to satisfy thermodynamic equilibrium.

UV–Vis Spectra

The UV–vis transmittance spectra of the PUA latex are given in Figure 7. Results indicate that the transmittance spectra of the PUA in the 700–200 nm wavelength range decreased as PU content increased. The reduction of transmittance in the visible light range results in the opaque film, which is consistent with the changes observed in the SEM of the film. These optical changes are caused by the quantity variations of PU. During the synthesis process, PU particles act as seeds and polymeric surfactants. Most AC monomers diffuse into the PU particles, which results in larger particle size after polymerization. Indeed, the introduction of PU into the systems significantly increases the composite latex size, yielding products of low transmittance. In addition, when PU content increases up to a certain point (at 10 wt %), the appearance of this emulsion is milky white and it renders the film opaque. However, for samples with 15 wt % of PU, the transmittance curves of the hybrid emulsions show an increment. This can be explained by that the excessive electrolyte generated by PU leads to decrease in the critical micelle concentration and lower particle size, resulting in increasing the transmittance of the hybrid emulsions.

Thermogravimetric Analysis

The decomposition curves of PU and PUA films with PU levels of 3–15 wt % are presented in Figure 8. Based on the experimental TGA, it is observed that the degradation of pure PU has three stages, while the PUA hybrids depict two stages of weight loss. It is clear that the PUA hybrids have higher thermal stability than that of the pure PU because the PUA hybrids showed higher degradation temperature, suggesting partial compatibility and interdiffusion of AC and PU. It is observed that the first stage thermal degradation of PUA took place at 150–230°C. Because the polyurethane linkages are cleaved at temperatures above 180°C, the loss of weight at temperatures under 180°C could be due to the elimination of water generated from further condensation process, which were not been released during the drying process. The second stage took place at ~350–400°C. This weight loss can be attributed to decomposition of the AC chain. The behavior followed from the presence of PU-AC linkages in the membranes, which increased the polymer degradation temperature by shifting the weight loss to higher

Table III. Contact Angle Values of Water for PUA Emulsion Latex

PU content (wt %)	3	5	7	10	15
Contact angle	60.3	60.6	74.9	43.9	50.8

temperatures. However, the thermal indexes for 10–15 wt % PU dropped because of the poor compatibility between AC and PU, which indicates that the interactions between the PU and the AC chains through H-bonds became weaker. As seen in Figure8(e) it could also be found that the PUA hybrid with 15 wt % of PU proceeds as a three step process, which might be resulted from the increasing phase separation between the two phases, and the middle stage probably due to the degradation of PU component which separated from the hybrids, since the pure PU is primarily degradation at this temperature region.

Contact Angle

The contact angle of water on the PUA film surface is shown in Table III, which directly indicates the hydrophilicity or hydrophobicity of the surface. The water surface contact angle on PUA was found to increase continuously from 60 to 74.9 as PU content increased from 3 to 7 wt %. The AC composites, including HEMA, MMA, BA, and St monomers, may provide more water resistance than PU. At low polyurethane concentration (3–7 wt %), PUA hybrid films exhibited hydrophobic properties because of good compatibility between AC and PU that they combine the positive properties of both polymers in a synergistic way, as evidenced by the increase of contact angle from 60.3° to 74.9°. However, at higher PU concentrations (10 wt %) this parameter decreases to lower values, which may be due to the poor phase compatibility between PU and AC domains, and the introduction of PU into a waterborn acrylic latex is expected to increase the hydrophilic properties because the PU contains many strong polar COOH groups. Moreover, the water contact angle is related to surface roughness. Wenzel[34] have demonstrated that a rough surface exhibiting high hydrophilic properties is expected to increase the contact area of the solid-liquid leading to a high wettability, a lower contact angle of the film can be obtained. In case of 15 wt % PU, a slight increment was observed as compared to 10 wt % PU which may be attributed to the benefits of the loosely hydrogen bond formed between self-associated urethane groups.

Table IV. Electrophoresis of PUA Composite Emulsion

Item	Property
Appearance	Smooth
Gloss	4.0
Film thickness (μm)	19–22
Adversity	1
Impact resistance (cm)	>50
Pencil hardness	3 H
Salt spray resistance (5% NaCl, 24 h)	Pass
Acid resistance (5% H_2SO_4, 72 h)	Pass
Alkali resistance (3%NaOH, 72 h)	Pass

Electrophoresis Properties

The properties of the electrophoresis film are shown in Table IV. In general, the film showed excellent mechanical performance and a gloss as low as 4.0, significantly lower than that of PUA film without electrophoresis. The curing reaction between hydroxyl group of AC with isocyanate groups of PU and enclosed water-based isocyanate crosslinking agent results in the crosslinked structure (Figure 2). This curing reaction provides an alternative for modifying properties of PUA films and forming a matting appearance on the aluminum samples.

CONCLUSIONS

Hybrid acrylic–polyurethane emulsions were synthesized in a semibatch process with different levels of PU by weight. The surface gloss, morphology, and comprehensive properties were found to change when different amounts of the PU component were present in the AC matrix. The structure of hybrid PUA was examined by FTIR, which confirmed the incorporation of the PU into AC composition. The physical properties and morphology of hybrid PUA were greatly influenced by PU concentration. When the PU concentration was at a low level (below 10 wt %), due to the better compatibility between PU and AC in the hybrid films, physical properties and thermal stability of the hybrid films were improved with the elevated PU concentration. In contrast, the physical properties and thermal stability decreased under the higher PU concentration (above 10 wt %) due to the slight phase separation between AC and PU, which confirmed by scanning electron microscopy. A tendency to uneven volume shrinkage was occurred during the drying process with high PU concentration, resulting in a roughness of film surface. Opaqueness of the hybrids was increased and matted surface was obtained. The roughness and morphology of the PUA latex films observed via SEM and the transmittance spectra recorded using the UV spectrum are closely consistent with the observed surface gloss. Transmission electron micrographs suggest the PUA hybrid systems are made up of particles with a core-shell structure. After neutralization with *N*,*N*-dimethylethanolamine, the typical particles formed a hydrated polymer shell surrounding with a unswollen core. The presence of MAA and the increasing fraction of PU can affect the interfacial tensions of the hybrid latex, which may provide driving force for phase separation and form irregular hemispheres to satisfy thermodynamic equilibrium.

From a practical point of view, the incorporation of PU into the AC matrix allows the production of materials with different final properties. These properties can be adjusted to the applications as needed. Further material development in electrophoresis with 10 wt % PU content was proceeded on aluminum profile, after drying at 120°C for 0.5 h, the aluminum profile showed excellent mechanical and chemical performance, and a gloss as low as 4.0 was obtained, indicating that this PUA hybrid emulsion could be useful in practical extinction electrophoresis. This study provides a new perspective on the matted materials by means of the PUA hybrid emulsions in electrophoresis and our further attention would be focused on the synthesis of high solid content emulsion for satisfactory application.

ACKNOWLEDGMENTS

The authors wish to acknowledge the assistance of Guangdong Province comprehensive strategic cooperation of the Chinese academy of sciences program (No. 2009B091300090) and Foshan City and the Chinese academy of sciences cooperation project (2012YS10).

REFERENCES

1. Okamoto, Y.; Hasegawa, Y.; Yoshino, F. *Prog. Org. Coat.* **1996**, *29*, 175.
2. Hirose, M.; Zhou, J. H.; Nagai, K. *Prog. Org. Coat.* **2000**, *38*, 27.
3. Hegedus, C. R.; Kloiber, K. A. *J. Coat. Technol.* **1996**, *68*, 39.
4. Hirose, M.; Kadowaki, F.; Zhou, J. H. *Prog. Org. Coat.* **1997**, *31*, 157.
5. Wu, L. M.; Yu, H. K.; Yan, J.; You, B. *Polym. Int.*, **2001**, *50*, 1288.
6. Kukanja, D.; Golob, J.; Krajnc, M. *J. Appl. Polym. Sci.* **2002**, *84*, 2639.
7. Wu, L. M.; You, B.; Li, D. *J. Appl. Polym. Sci.* **2002**, *84*, 1620.
8. Kukanja, D.; Golob, J.; Zupancic-Valan, A.; Krajnc, M. *J. Appl. Polym. Sci.* **2000**, *78*, 67.
9. Sebenik, U.; Golob, J.; Krajnc, M. *Polym. Int.*, **2003**, *52*, 740.
10. Lopez, A.; Degrandi-Contraires, E.; Canetta, E.; Creton, C.; Keddie, J. L.; Asua, J. M. *Langmuir* **2011**, *27*, 3878.
11. Kim, I. H.; Shin, J. S.; Cheong, I. W.; Kim, J. I.; Kim, J. H. *Colloids Surf. A Physicochem. Eng. Aspects* **2002**, *207*, 169.
12. Nabuurs, T.; Baijards, R. A.; German, A. L. *Prog. Org. Coat.* **1996**, *27*, 163.
13. Wang, S. T.; Schork, F. J.; Poehlein, G. W.; Gooch, J. W. *J. Appl. Polym. Sci.* **1996**, *60*, 2069.
14. Wu, X. Q.; Schork, F. J.; Gooch, J. W. *J. Polym. Sci. Part A: Polym. Chem.* **1999**, *37*, 4159.
15. de Wet-Roos, D.; Knoetze, J. H.; Cooray, B.; Sanderson, R. D. *J. Appl. Polym. Sci.* **1999**, *71*, 1347.
16. Kawahara, H.; Goto, T.; Ohnishi, K.; Ogura, H.; Kage, H.; Matsuno, Y. *J. Appl. Polym. Sci.* **2001**, *81*, 128.
17. Wang, C.; Chu, F.; Graillat, C.; Guyot, A. *Polym. React. Eng.* **2003**, *11*, 541.
18. Wang, C.; Chu, F.; Graillat, C.; Guyot, A.; Gauthier, C. *Polym. Adv. Technol.*, **2005**, *16*, 139.
19. Aznar, A. C.; Pardini, O. R.; Amalvy, J. I. *Prog. Org. Coat.* **2006**, *55*, 43.
20. Zhou, X. H.; Tu, W. P.; Hu, J. Q. *Chin. J. Chem. Eng.* **2006**, *14*, 99.
21. Gite, V. V.; Mahulikar, P. P.; Hundiwale, D. G. *Prog. Org. Coat.* **2010**, *68*, 307.
22. Guo, Y. H.; Li, S. C.; Wang, G. S.; Ma, W.; Huang, Z. *Prog. Org. Coat.* **2012**, *74*, 248.
23. Sebenik, U.; Krajnc, M. *J. Polym. Sci. Part A: Polym. Chem.* **2005**, *43*, 4050.
24. Sebenik, U.; Krajnc, M. *J. Polym. Sci. Part A: Polym. Chem.* **2005**, *43*, 844.
25. Kajtna, J.; Likozar, B.; Golob, J.; Krajnc, M. *Int. J. Adhes. Adhes.* **2008**, *28*, 382.
26. Zheng, J.; Shen, T. F.; Ma, J. Y.; Liang, L. Y.; Lu, M. G. *Chem. Phys. Lett.* **2011**, *502*, 211.
27. Athawale, V. D.; Kulkarni, M. A. *Prog. Org. Coat.* **2009**, *65*, 392.
28. Segall, I.; Dimonie, V. L.; Elaasser, M. S.; Soskeyand, P. R.; Mylonakis, S. G. *J. Appl. Polym. Sci.* **1995**, *58*, 401.
29. Slisenko, O. V.; Grigor'eva, O. P.; Starostenko, O. N.; Sukhorukov, D. I.; Lebedev, E. V. *Polym. Sci. Ser. A* **2006**, *48*, 809.
30. Huang, X. B.; Ren, T. B.; Tang, X. Z. *Mater. Lett.* **2003**, *57*, 4182.
31. Zhang, Q. H.; Yang, Z. B.; Zhan, X. L.; Chen, F. Q. *J. Appl. Polym. Sci.* **2009**, *113*, 207.
32. Sundberg, D. C.; Durant, Y. G. *Polym. React. Eng.* **2003**, *11*, 379.
33. Goikoetxea, M.; Reyes, Y.; Alarcon, C. M. D.; Minari, R. J.; Beristain, I.; Paulis, M.; Barandiaran, M. J.; Keddieand, J. L.; Asua, J. M. *Polymer* **2012**, *53*, 1098.
34. Wenzel, R. N. *J. Phys. Colloid Chem.* **1949**, *53*, 1466.